ATMOSPHERIC ENVIRONMENT: X 16 (2022) 100189

Contents lists available at ScienceDirect

Atmospheric Environment: X

journal homepage: www.journals.elsevier.com/atmospheric-environment-x

Particle number, mass, and black carbon emissions from fuel-operated auxiliary heaters in real vehicle use

Henri Oikarinen [a], Miska Olin [b], Sampsa Martikainen [b], Ville Leinonen [a], Santtu Mikkonen [a,c], Panu Karjalainen [b,*]

[a] Department of Applied Physics, University of Eastern Finland, P.O.B. 1627, 70211, Kuopio, Finland
[b] Aerosol Physics Laboratory, Tampere University, P.O.B. 692, 33014, Tampere, Finland
[c] Department of Environmental and Biological Sciences, University of Eastern Finland, P.O.B. 1627, 70211, Kuopio, Finland

ARTICLE INFO

Keywords:
Auxiliary heaters
Particle formation
Emissions
Cold start emissions
Passenger cars
Traffic
Vehicles
Exhaust emissions
Combustion
Black carbon
Particle size distribution
Vehicle cold start
PM
Soot formation
Particle number
Emission factor

ABSTRACT

Fuel-operated auxiliary heaters (AHs) are frequent solutions to heat the vehicle engines and cabins in cold areas. Particulate exhaust emissions of AHs are unregulated; therefore, their contribution to local air quality and thus human health and even the global emissions budget is unknown. Experiments for studying the AH-originated emissions were performed under Finnish winter conditions mimicking real-world use for six selected vehicles with original AHs installed, including both gasoline- and diesel-powered heaters. We present quantitative results of particle number emissions down to 1.3 nm, particle size distributions, particulate mass, and black carbon, and compare to gaseous emissions. The start-up and shutdown phases showed the highest particle peaks, while the particle concentrations were stable between these. The mean particle number, mass and BC emission factors were found to be as high as 590×10^{12} kg_{fuel}^{-1}, 33 mg kg_{fuel}^{-1} and mg 18 kg_{fuel}^{-1} for gasoline-operated heaters and 560×10^{12} kg_{fuel}^{-1}, 20 mg kg_{fuel}^{-1} and 12 mg kg_{fuel}^{-1} for diesel-operated heaters. Comparing total number of particles larger than 23 nm emitted during vehicle preheating with AH to vehicle tailpipe emissions during drive shows that a typical heating cycle emits an equal number of particles to drive dozens or even thousands of kilometers.

1. Introduction

Major human-induced environmental challenges include poor air quality and the acceleration of climate change. Traffic-originated emissions are a significant factor in both. Exposure to airborne respirable particles, meaning particulate matter below 2.5 μm in size (PM2.5) is an immense global challenge estimated to cause approximately 4.2–8.9 million premature deaths per year worldwide (Burnett et al., 2018; Chowdhury et al., 2022). In addition, aerosols are an important anthropogenic component affecting global warming by contributing to Earth's radiation balance with high uncertainties (Forster et al., 2021). In an urban environment, traffic exhaust fumes are one of the most significant sources of aerosol particles and precursor gases affecting new particle formation in the air. The main components of traffic-originated particles are black carbon (BC), as well as primary and secondary organic aerosols (Gentner et al., 2017). The composition and size distributions of particles vary greatly between emission sources and ageing state (Gentner et al., 2017). Combustion-originated particles can transport long distances and affect, e.g., cloud formation and surface albedo especially on snowy and icy surfaces (Hadley and Kirchstetter, 2012).

Due to the adverse effects, the tailpipe emissions of vehicles are under emission regulations. More stringent emission limits are constantly being legislated. In some cases, mass emissions have reduced near to the detection limit of gravimetric method (Giechaskiel et al., 2014). However, mass may not be the best measure for adverse health effects (Hadley and Kirchstetter, 2012); therefore, the updates in regulatory particle emission limits have introduced a particle number (PN) limit. In Europe, the PN emission levels of non-volatile particles for light-duty diesel vehicles have been implemented since 2009 (Dieselnet, 2015). Additionally, starting from Euro 6 emission standards implemented in 2014, non-volatile exhaust PN has been regulated for gasoline

* Corresponding author.
E-mail address: panu.karjalainen@tuni.fi (P. Karjalainen).

https://doi.org/10.1016/j.aeaoa.2022.100189
Received 21 March 2022; Received in revised form 1 July 2022; Accepted 23 September 2022
Available online 24 September 2022

Abbreviations

AE	Aethalometer
AH	Auxiliary Heater
BC	Black Carbon
CPC	Condensation Particle Counter
DR	Dilution Ratio
DPF	Diesel Particulate Filters
EEPS	Engine Exhaust Particle Sizer
EF	Emission Factor
FID	Flame Ionization Detector
GMD	Geometric Mean Diameter
NO_x	Nitrous Oxides
OBD	On-Board Diagnostics
PM	Particulate matter
PN	Particulate number
SOA	Secondary Organic Aerosol
THC	Total Hydrocarbons
WLTC	Worldwide harmonized Light vehicles Test Cycle

direct injection passenger cars. This non-volatile particle regulation currently includes particles larger than 23 nm in size and stands at 6×10^{11} km^{-1}. The PN limit for diesel passenger cars has de facto enforced the use of diesel particulate filters (DPFs) in the exhaust line. These filters have been shown to be very efficient in PN reduction, e.g., reduction efficiency of up to 99.998% has been reported (Wihersaari et al., 2020).

When a vehicle engine is started after a long parking time under sub-zero conditions or close to them, preheating of the engine, vehicle body and cabin are preferred. This originates from various aspects, such as prevention of engine wear right after the cold start, melting the accumulated ice from the vehicle windows, warming up the ventilation air to reduce fogging of windshield, and increasing passenger comfort. Typical strategies to heat up the engine include starting the engine and holding it on idle for several minutes or using an external heating source before the engine start-up. The latter is often intended to reduce engine wear under very cold weather conditions and to ensure successful engine starting. External heaters can be electrically operated – having a drawback of the requirement of the power grid connection – or they can be fuel-burning auxiliary heaters (AHs) providing higher power output and more freedom for the selection of the parking location. Additionally, fuel-operated AHs often activate during normal operation of the vehicle after cold start to increase the heating rate of the engine, exhaust after-treatment system, and cabin. In some vehicles, manual usage of the heater is impossible; instead, it automatically activates during the vehicle start under cold conditions. Fuel-operated AHs use the same fuel tank as the internal combustion engine, but they have a separate short exhaust pipe right below the heating unit close to the engine. AHs are common solutions in cold regions to heat up the engine and cabin in diesel and gasoline passenger cars, gasoline hybrids, trucks, and buses, even in electrical ones. Karjalainen et al. (2021) reported that the annual sales of the two major AH manufactures exceed one billion EUR, but the total number of sold devices is not available from public sources. However, we can assume that the global number of devices in use is in the order of tens, if not hundreds, of millions.

Unlike vehicle exhaust, the AH exhaust emissions are less regulated since it is an additional heat source, not the source of driving power. The AH exhaust regulation concerns loose concentration limits for carbon monoxide (max 0.1%), nitrogen oxides (NO_x; max 200 ppm) and total hydrocarbons (THC; max 100 ppm) under stable flame conditions targeting only safe air quality for the passengers (EUR-Lex, accessed 3.2.2022), and not considering the particle emissions and environmental effects of the AH exhaust. Fuel-operated AHs can be a large source of particle emissions that cannot easily be distinguished in air quality measurements in traffic environments. This was demonstrated for the first time in a recent brief report (Karjalainen et al., 2021) where the particle number concentrations of both gasoline and diesel operated AHs were seen to be significantly higher than the concentrations from the passenger vehicle running on idle for the same time period. Studying the aerosol emissions from fuel operating auxiliary heaters has been almost neglected in the scientific literature, as the earlier studies have mainly focused on improving the thermal efficiency or decreasing the fuel consumption of heaters (Müller et al., 2009). Contrariwise, modified AHs have been applied as soot particle generators in laboratory studies (Högström et al., 2012).

In this article, we show that AHs can be significant sources of particle emissions in their real use. Experiments were performed in Finland under cold winter conditions for a total of 6 selected in-use vehicles having AHs installed. Both diesel and gasoline vehicle technologies were covered. We present the experimental findings of PN & particulate mass (PM) emissions, particle size distributions, and the concentrations of black carbon (BC), carbon dioxide (CO_2), NO_x, and THC. We analyzed the phenomena related to emission formation at different stages of the AH heating cycle and report realistic emission factors for the studied components.

2. Materials and methods

2.1. Test matrix and measurement protocol

Information about the vehicles, their AHs and the measurement setup is presented in Fig. 1. The test matrix included six vehicles in total, three of which were operated with gasoline and three with diesel. All AHs were OEM devices, manufactured by Webasto Ltd, but for the diesel BMW the original heater was replaced to the identical, used spare part some years ago. Their exact runtimes could not be defined with the OBD instrumentation in use but the runtime is expected to be proportional to vehicle mileage. The used gasoline fuels were of the 95E10 grade (95 octane, max 10% ethanol), and the diesel fuels met the EN 590 (min 7% renewable) standard. The AHs used the same fuel as the vehicles they were installed in. The tests were conducted within four consecutive days under Finnish winter conditions (−19 to −7 °C), meaning each AH was measured four times. The measurement protocol included an overnight cooling period of over 18 h, after which the vehicle was driven from the parking slot to the sampling location (both outdoors, open air). This transfer was kept as brief as possible (less than 20 s), to prevent excessive engine heating and automatic starting of the AH. After attaching the sampling line to the exhaust pipe of the AH, the heater was turned on and left to run for about 30 min. Both the total run time and the general operation pattern of the AHs varied between the vehicles. Some AHs ran steadily for the predetermined heating time until manual shutdown, whereas some periodically turned on and off and others shut down automatically before the 30-min mark was reached. Parameters describing the operation of the heater were recorded using on-board diagnostics.

2.2. Sampling

The sampling was performed with a dilution system (Fig. 1) consisting of a porous tube diluter (PTD), a residence time tube, and an ejector diluter. The system was originally developed to mimic the dilution, cooling and subsequent particle formation processes the exhaust aerosol undergoes in the surrounding air after exiting the vehicle tailpipe (Ntziachristos et al., 2004). In other words, it allows the semivolatile compounds to condense on the pre-existing exhaust particles or to form new particles via nucleation. This type of dilution system has been calibrated to characterize the real-world particle emissions of vehicles with respect to nucleation mode formation (Rönkkö et al., 2006), and has been extensively applied in several exhaust studies (e.g.

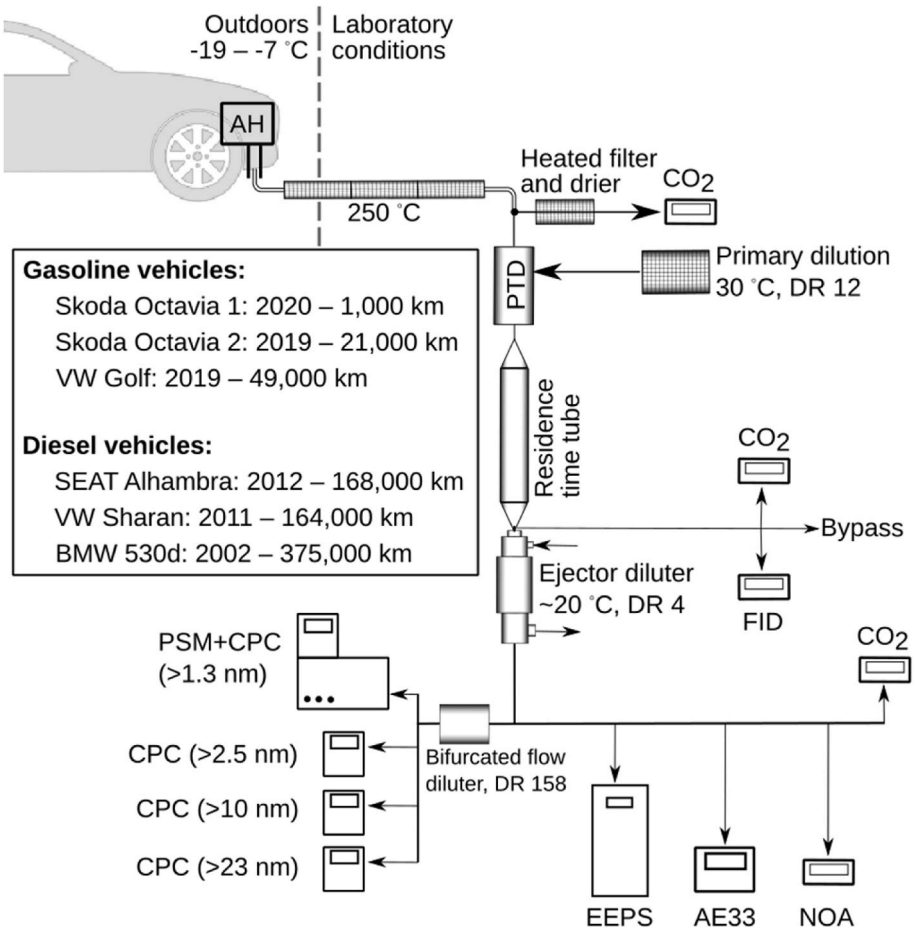

Fig. 1. Measurement setup consisted of a heated sampling line, PTD dilution system and aerosol instrumentation. Test vehicles with their registration years and odometer readings are also shown. (1 column).

Karjalainen et al., 2014; Keskinen and Rönkkö, 2010; Rönkkö et al., 2007). The 3-m-long sampling line leading from the exhaust pipe of the AH to the PTD was heated to 250 °C. The test vehicle was left outdoors whereas the measurement instruments were kept in warm indoors conditions. The dilution ratio (DR) of the PTD was adjusted to 12 according to CO_2 concentrations measured from the raw exhaust and after the dilution. The PTD dilution air temperature was set to its nominal value of 30 °C. The smoke from the exhaust was visible, especially in the case of heater startup. The smoke was whitish in color, and possibly including condensed and later frozen water on top on the original aerosol. Under stabilized combustion conditions, the smoke was not that visible at all. The AH exhaust line is very short after the heater, in the order of 15–20 cm. We did not observe condensates on the heater exhaust line surfaces.

2.3. Instruments

Several aerosol properties were measured from the sample. Particle number concentration and size distribution, BC mass concentration, CO_2 concentration, NO_x concentration and THC concentration were measured with Condensation Particle Counters (CPCs; CPC 3756, TSI Inc.; PSM A10 + CPC A20, CPC A20, CPC A23, Airmodus Ltd), an Engine Exhaust Particle Sizer (EEPS, TSI Inc.), an Aethalometer (AE33, Aerosol Co.), CO_2 analyzers, a NO_x analyzer (Teledyne Model T201), and a Flame ionization detector (FID, Mocon Baseline 9000), respectively. CPCs used in the measurement of number concentration had different cut-off sizes (1.3, 2.5, 10 and 23 nm). CO_2 concentration was measured from the raw exhaust (SIDOR, SICK AG), as well as downstream every dilution step (2 × LI-COR LI-840 A). Upstream the CPCs, a bifurcated flow diluter was installed to keep the concentration level suitable for the instruments.

2.4. Data processing

Overall aim of the data processing was matching measured emission data with actual emissions at the end of the AH exhaust pipe. Emission data collected from the measurement devices were corrected to remove effects of dilution, diffusion, and the bifurcated flow diluter in the measurement setup. DR of each dilution step for each separate AH measurement was calculated by dividing the mean of measured CO_2 concentration before dilution by the mean of CO_2 concentration after dilution. For the bifurcated flow diluter, DR was assumed to be equal to an experimentally verified constant of 158. In the EEPS data processing, the inversion matrix for soot particles (Wang et al., 2016) was applied. The diffusion losses in the sampling were corrected for EEPS and CPCs. The CPC readings were also corrected with calibration values obtained just prior the experiments. BC and THC concentration time series were also filtered with a modified Hampel filter to remove spike artifacts from the time series (Pearson et al., 2016). To ease the comparison of different measurement devices, timestamps of the time series were synchronized due to different residence times in the sampling lines. AHs were assumed to operate in full or partial power with exception of short ignition and shutdown periods in the beginning of and at the end of the heating cycle, respectively. Gasoline-powered AHs were assumed to operate by a constant 5 kW heating power during stable part of the heating cycle, with manufacturer-given fuel consumption of 0.7 l/h, while

diesel-powered AHs were assumed to operate by constant 5 kW heating power during most of heating cycle with manufacturer-given fuel consumption of 0.62 l/h, with a possibility of a 2.5 kW partial power with manufacturer-given fuel consumption of 0.31 l/h, at the end of heating cycle. In addition to the fuel consumptions reported by the manufacturer, their correctness was ensured by checking the readings of the consumptions via the OBD instrumentation for two diesel vehicles.

2.5. Emission factor calculations

To compare the relative emission profiles of the vehicles, emission factors (EFs) were calculated by taking the time integral of the measured concentration over the entire heating cycle and dividing by the time integral of CO_2 mass concentration from the same period. EFs were further normalized with respect to heating time by either extending or shortening the plateau part of the measured cycle to make the entire heating cycle exactly 30 min long. Time-normalized EFs are also given for 1 min of heating during the plateau of the cycle, except for BMW 530 d, for which the 1-min EF is calculated from the first on-off cycle. The 1-min EF is indicative of change in heating emissions caused by extending or shortening the heating period. Additionally, average EFs for each vehicle, as well as for all diesel and gasoline vehicles, are calculated. EF calculations relied on first calculating total emissions of a heating cycle (E) from EFs by taking the amount of fuel consumed during the heating cycle into account. Equation used in total emission calculation is presented below

$$E = \frac{\int_0^t [E]dt}{\int_0^t [CO_2]dt} K t \rho \frac{m_{C,fuel}}{m_{tot,fuel}} \frac{M_{CO_2}}{M_c}$$

where $[x]$ (kg or # per m^3) is measured concentration of substance, t (h) is duration of heating cycle, K (l/h) is fuel consumption rate of AH, ρ(0.740 kg/l for gasoline and 0.805 for diesel) is density of fuel, $m_{C,fuel}/m_{tot,\ fuel}$ is carbon mass fraction of fuel and M_{CO2}/M_C is ratio of mass increase when carbon in fuel is transformed into CO_2 and released in combustion. Total emissions E emission factor relative to fuel consumption were calculated by simple division with mass of consumed fuel. EFs relative to heating time of either 30 or 1 min are simply total emission E for respective duration of AH heating.

3. Results and discussion

Operation of the AHs varied over the heating cycle and especially diesel heaters showed a tendency to limit or stop combustion during operation. In Fig. 2, an example of a complete heating cycle from the diesel-powered AH of SEAT Alhambra is presented. Effects of a single complete heating cycle to exhaust CO_2 concentrations and engine coolant temperatures are shown. From the start, it took 1–2 min for CO_2 concentrations to rise to the stable level of ~8% (volumetric). As observed from Fig. 2, heating of the coolant liquid takes time. From the startup, the temperature increased from −10 °C to the asymptotic value of +67 °C gradually within 25 min. Notably, this vehicle can reduce the heating power of the AH when the coolant temperature has reached its nominal target temperature. Gasoline-powered AHs generally operated with a constant power during the heating cycle. There are also differences in the heating procedures of AHs in different vehicles on the market, of which some models heat the cabin first and subsequently the engine, whereas some heat them simultaneously and others even neglect the engine heating completely.

3.1. Particle number concentrations

In Fig. 3, the time series of PN concentrations during the heating cycle for all 6 vehicles are presented (data of single day). Most particles were larger than 10 nm in diameter with a small fraction of the particles in the range between 1.3 and 2.5 nm. Initial ignition and switching the AHs off caused high PN values while the middle parts of the heating cycles were relatively constant for most vehicles, excluding VW Golf for which the constant plateau was higher in the PN concentration compared to the ignition. Variance in temporal AH operation of different vehicles can also be seen in Fig. 3. Especially the AH of BMW repeatedly switched on and off during the heating cycle. This reduces the total fuel consumption with the cost of increased relative aerosol emissions due to a lack of stable combustion period. Number concentrations during the stable combustion periods also differed between the fuel types. For

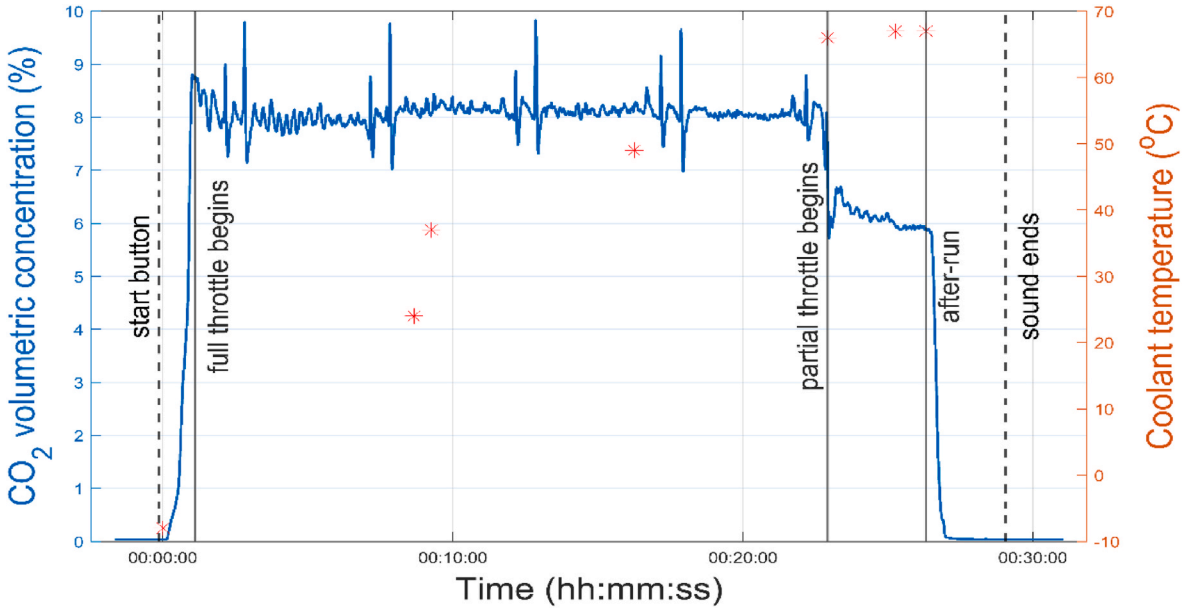

Fig. 2. Example AH heating cycle from SEAT Alhambra, showing the CO_2 concentration and coolant temperature (marked with asterisk) of the vehicle. Different parts of the heating cycle retrieved from the vehicle's on-board diagnostics are marked with solid vertical lines and auditory indication of cycle completion is marked with dashed vertical line. (1 column).

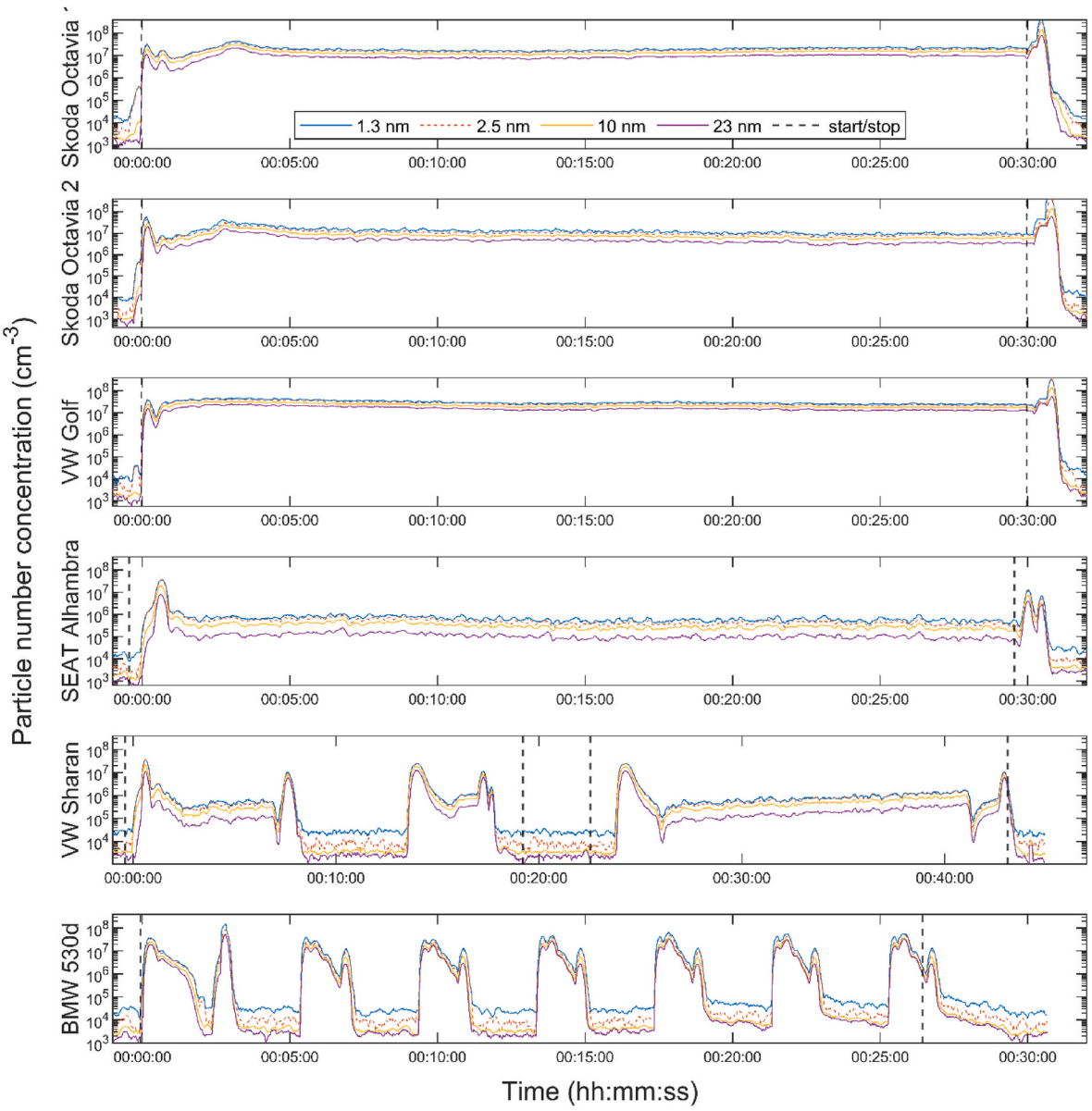

Fig. 3. Time series of particle number concentrations measured with CPCs with cut-off diameters of 1.3 nm, 2.5 nm, 10 nm, and 23 nm. The dashed vertical lines denote the times of pressing start and stop buttons of the AHs. The AH of VW Sharan was rebooted during its second shut-down period in the middle of the measurement due to irregularities in its operation. (2 column).

diesel-powered AHs the number concentrations during the stable periods were roughly 2 orders of magnitude lower compared to the peaks, while for gasoline-powered AHs the differences between the peaks and the stable periods were roughly 1 order of magnitude.

3.2. Particle size distributions

A more detailed look into particle size distributions can be gained from the EEPS, which classifies particles to 32 size bins within the size range between 5.6 and 560 nm. It should be noted that, firstly, the smallest particles cannot be observed with EEPS and, secondly, coagulation inside the sampling lines, especially within the first sampling line containing the undiluted sample, affects the measured sample so that the smallest particles cannot be observed (see Supporting Information), affecting potentially also PN results shown in Fig. 3. Hence, the reported size distributions may have slightly overestimated particle sizes and underestimated number concentrations, especially for the lowest particle sizes. However, the effect of coagulation is not corrected in the reported data since it cannot be unambiguously corrected afterwards. In Fig. 4, particle size distribution and geometric mean diameter (GMD) from EEPS is shown for all vehicles. Notable changes in particle size distribution can be seen during the ignition and shutdown periods with all vehicles compared to plateau size distribution. Additionally, gasoline-powered AHs show a burst of sub-20 nm particles at the last moments of AH shutdown, as can be seen from the sudden drop of GMD before the return to background particle size distribution. We assume that the start-up peak in concentration is caused by nonoptimal conditions during the cold start of the AH, including effects of developing air-to-fuel ratio in the combustion chamber. The plateau is the time for stable burning in conditions somewhat optimized for air-to-fuel ratio, thus showing stable emission profile. The end-peak is caused by rapid changes in air and fuel flows in the device and may also contain remained fuel in the combustion chamber that gets released in an unorthodox manner.

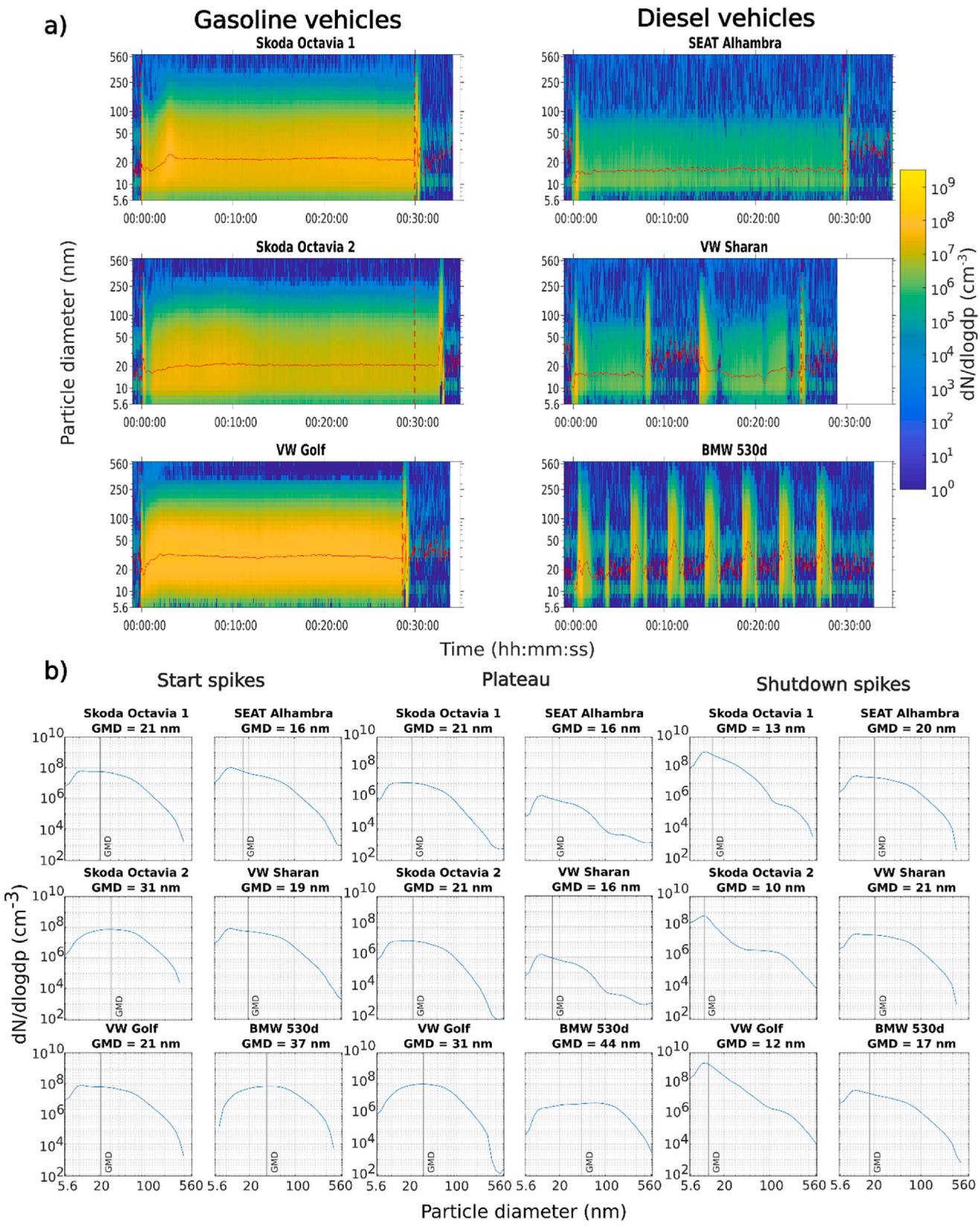

Fig. 4. a) Time series of particle size distributions measured with EEPS during the heating cycle. Geometric mean diameters are presented with red lines. AH ignition and stop button presses are marked with dashed vertical red lines on each subfigure. b) Cross sections of particle size distribution time series during peaks of start and shutdown spikes and also for time averaged size distributions during plateau portions of heating cycle. Geometric mean diameters are marked with vertical black lines. (2 column). (For interpretation of the references to color in this figure legend, the reader is referred to the Web version of this article.)

3.3. Emission factors

Averaged EFs for emissions of BC, PNs of particles larger than 1.3, 2.5, 5.6, 10 and 23 nm are provided along with mass concentration from EEPS size distribution and for NO_x and THC EFs in Table 1. Associated standard deviations reflect differences between the means of repeated measurements. Standard deviations for concentrations and EFs in Table 1 were also calculated from each individual heating cycle's internal variances, which are presented in Table S1 in Supporting Information. Average EFs for particulate emissions from gasoline vehicles are higher compared to diesel vehicles. The largest difference is for larger particles (>23 nm), having 4.6-fold EF for the gasoline vehicles compared to the diesel vehicles per 1 kg of fuel combusted. The difference is smaller when smaller particles are included (1.1-fold EF for >1.3 nm) or considering particle mass (1.7-fold EF). For gaseous emissions, EFs for different fuel types are relatively similar. For NO_x, the gasoline vehicles have on average 1.1-fold EFs compared to the diesel vehicles, and for THC the diesel vehicles have 2.8-fold EFs. However, the difference in THC is mostly explained by the high EF of BMW 530 d. We must note that the gasoline AHs were newer than diesel AHs which can have an effect on the results comparison.

EFs between the cars vary a lot. Notably BMW 530 d has significantly larger EFs compared to the other diesel vehicles due to the AH continuously switching on and off during the heating cycle. Also, for the relatively steady-operating gasoline-powered AHs, there is large variation between the vehicles, VW Golf having the largest EFs. Emission factors of NO_x and THC are relatively similar between the vehicles, with again notable deviation from the norm by BMW 530 d. The deviation of the NO_x emissions of BMW could be explained by NO_x formation in flames being a temperature dependent process (Glarborg et al., 2018), and with continuous on-off switching resulting in lower total NO_x emissions due to lower average AH temperature during heating.

Table 1
Average concentrations and emission factors of AH exhaust for all six vehicles and the averaged ones (standard deviation in parentheses) over the vehicles with the same fuel type. Emission factors are given per kilogram of fuel combusted, per a 30 min heating cycle and per 1 min of heating during a stable part of the cycle. Number of repeated measurements for all instruments besides CPCs was 4, for CPCs $PN_{>1.3\ nm}$ had 1 measurement for diesel-powered AHs and 2 for gasoline-powered AHs, while $PN_{>2.5\ nm}$ has 1 measurement for all vehicles. For measurements with only a single repetition, the lack of standard deviation is indicated by N/A.

Quantity (device)	Units	Skoda Octavia 1	Skoda Octavia 2	VW Golf	SEAT Alhambra	VW Sharan	BMW 530 d	Gasoline vehicles	Diesel vehicles
$PN_{>1.3\ nm}$ (CPC)	10^6/cm^3	16 (4)	8.4 (5.4)	44 (16)	0.88 (N/A)	1.8 (N/A)	6.6 (N/A)	23 (10)	3.1 (N/A)
	10^{12}/kg (fuel)	460 (180)	340 (250)	960 (360)	62 (N/A)	210 (N/A)	1400 (N/A)	590 (280)	560 (N/A)
	10^{12}/30min	120 (46)	89 (67)	250 (96)	15 (N/A)	51 (N/A)	180 (N/A)	150 (75)	82 (N/A)
	10^{12}/min	3.8 (1.6)	2.4 (1.9)	8.2 (3.3)	0.15 (N/A)	0.34 (N/A)	7.0 (N/A)	4.8 (2.4)	2.5 (N/A)
$PN_{>2.5\ nm}$ (CPC)	10^6/cm^3	17 (N/A)	12 (N/A)	24 (N/A)	0.74 (N/A)	1.7 (N/A)	4.9 (N/A)	17 (N/A)	2.5 (N/A)
	10^{12}/kg (fuel)	420 (N/A)	270 (N/A)	540 (N/A)	27 (N/A)	89 (N/A)	520 (N/A)	410 (N/A)	210 (N/A)
	10^{12}/30min	110 (N/A)	72 (N/A)	140 (N/A)	6.9 (N/A)	22 (N/A)	67 (N/A)	110 (N/A)	32 (N/A)
	10^{12}/min	3.6 (N/A)	2.1 (N/A)	4.4 (N/A)	0.092 (N/A)	0.19 (N/A)	2.4 (N/A)	3.4 (N/A)	0.9 (N/A)
$PN_{>10\ nm}$ (CPC)	10^6/cm^3	9.8 (2.8)	4.8 (2.9)	27 (8.8)	0.57 (0.14)	1.2 (0.044)	2.6 (0.92)	14 (5.6)	1.4 (0.54)
	10^{12}/kg (fuel)	240 (75)	110 (63)	610 (190)	19 (4.1)	54 (2.3)	210 (140)	320 (120)	94 (83)
	10^{12}/30min	62 (20)	29 (17)	160 (51)	4.5 (0.83)	13 (0.40)	29 (16)	84 (33)	16 (9.4)
	10^{12}/min	1.9 (0.71)	0.81 (0.53)	5.2 (1.7)	0.054 (0.0028)	0.16 (0.044)	1.4 (0.29)	2.7 (1.1)	0.52 (0.17)
$PN_{>23\ nm}$ (CPC)	10^6/cm^3	6.2 (2.1)	2.8 (1.9)	21 (7.3)	0.27 (0.1)	0.67 (0.0033)	1.9 (0.87)	9.9 (4.5)	0.96 (0.51)
	10^{12}/kg (fuel)	140 (56)	58 (37)	460 (160)	6.9 (1.9)	24 (2.5)	110 (74)	220 (100)	48 (43)
	10^{12}/30min	38 (15)	15 (9.9)	120 (42)	1.7 (0.39)	5.9 (0.55)	16 (8.1)	58 (26)	7.9 (4.7)
	10^{12}/min	1.2 (0.50)	0.47 (0.33)	3.9 (1.4)	0.02 (0.00098)	0.067 (0.017)	0.69 (0.080)	1.9 (0.90)	0.26 (0.047)
$PN_{>5.6\ nm}$ (EEPS)	10^6/cm^3	15 (5.2)	10 (4.3)	45 (12)	0.88 (0.24)	1.9 (0.39)	4.5 (1.1)	23 (7.7)	2.4 (0.69)
	10^{12}/kg (fuel)	340 (130)	220 (87)	1000 (250)	25 (4.8)	65 (20)	270 (97)	530 (170)	120 (57)
	10^{12}/30min	88 (34)	58 (23)	270 (65)	6.1 (1.2)	16 (4.8)	38 (10)	140 (44)	20 (6.6)
	10^{12}/min	2.7 (1.2)	1.7 (0.77)	8.7 (2.2)	0.085 (0.032)	0.25 (0.026)	1.4 (0.22)	4.4 (1.5)	0.57 (0.13)
PM (EEPS)	mg/m^3	0.44 (0.18)	0.38 (0.13)	1.9 (0.64)	0.068 (0.034)	0.11 (0.038)	0.63 (0.21)	0.91 (0.39)	0.27 (0.12)
	mg/kg(fuel)	12 (5.5)	9.2 (3.8)	78 (46)	1.9 (0.77)	5.7 (1.3)	53 (25)	33 (27)	20 (15)
	mg/30min	3.2 (1.5)	2.4 (1.0)	21 (12)	0.46 (0.18)	1.4 (0.31)	7.3 (3.0)	8.7 (7.2)	3.1 (1.7)
	mg/min	0.24 (0.090)	0.084 (0.042)	1.2 (0.82)	0.009 (0.0023)	0.078 (0.0035)	0.22 (0.10)	0.51 (0.48)	0.1 (0.059)
BC (AE33)	mg/m^3	0.32 (0.16)	0.27 (0.12)	1.8 (0.64)	0.013 (0.0056)	0.039 (0.02)	0.58 (0.21)	0.79 (0.43)	0.21 (0.12)
	mg/kg(fuel)	7.3 (3.9)	5.8 (2.5)	40 (15)	0.37 (0.18)	1.5 (0.83)	35 (15)	18 (9.3)	12 (8.9)
	mg/30min	1.9 (1.0)	1.5 (0.65)	10 (4.0)	0.087 (0.039)	0.36 (0.20)	4.8 (1.8)	4.6 (2.4)	1.8 (1.1)
	mg/min	0.053 (0.035)	0.029 (0.014)	0.31 (0.14)	−0.00022 (0.00057)	0.0059 (0.0056)	0.12 (0.020)	0.13 (0.085)	0.04 (0.012)
NO_x (NOA)	ppm	95 (6.9)	100 (5.9)	96 (4.8)	68 (4.5)	54 (8.8)	31 (10)	97 (6.0)	51 (8.1)
	mg/kg(fuel)	4200 (150)	4100 (110)	4200 (140)	3900 (47)	3900 (95)	3100 (170)	4100 (130)	3600 (110)
	mg/30min	1100 (40)	1100 (41)	1100 (37)	940 (30)	950 (32)	480 (110)	1100 (39)	790 (70)
	mg/min	37 (1.3)	36 (1.8)	37 (1.3)	31 (0.61)	32 (0.78)	12 (0.89)	37 (1.5)	25 (0.77)
THC (FID)	ppm	26 (2.5)	23 (3.6)	29 (8.8)	25 (0.82)	29 (1.7)	60 (9.9)	26 (5.7)	38 (5.8)
	mg/kg(fuel)	1100 (87)	920 (170)	1200 (400)	1400 (48)	1600 (700)	6400 (2100)	1100 (250)	3100 (1300)
	mg/30min	280 (23)	240 (39)	320 (100)	330 (12)	380 (170)	910 (200)	280 (68)	540 (150)
	mg/min	5.8 (0.38)	4.4 (0.23)	5.4 (0.40)	7.7 (0.76)	12 (4.1)	23 (4.4)	5.2 (0.35)	15 (3.5)

Relatively higher THC emissions of BMW result possibly from impure combustion being extended by continuous on-off switching. The ratio of the mass of all particles detected by EEPS and BC particles measured with AE33 has high variability between the measurement days and vehicles. The ranges of the BC fractions were 12–62% for Octavia 1, 33–54% for Octavia 2, 81–97% for Golf, 73–98% for Alhambra, 52–86% for Sharan, 46–83% for 530 d, 12–97% for gasoline vehicles overall, and 46–98% for diesel vehicles overall. The reason for differing emission profiles is not certain. For example, even though the devices in two Octavias and Golf are of the same model and the fuel should be of the same standard, the emission profiles differ highlighting the significant variability of different individual units in real use. If the BC emission factors are compared to vehicle emissions, reported e.g. inWang et al., 2018, it can be noted that the EF for AHs are lower than for older diesel vehicles, with no DPF, but notably higher than for newer diesel or gasoline engines.

3.4. Comparison with vehicle driving emissions

The particle emissions of AHs are next compared to emissions from real driving. The limit for the particle number emissions of non-volatile particles larger than 23 nm in the current European regulation stands at 6×10^{11} 1/km. The EFs determined from the AH measurements with the CPC >23 nm were compared against the assumed driving emissions in Table 2. The baseline assumption is that the driving emissions are equal to the limit in the regulation. In reality, particle number emissions can be orders of magnitude lower or higher than the limit. For example, emissions less than the limit can be met with vehicles equipped with particulate filters. Conversely, emissions more than the limit can be met with vehicles with removed or malfunctioning filters or with older vehicles not yet incorporated in particle number regulations. Additionally, higher emissions can be met in real driving situations, e.g., in cold atmosphere, where particle number emissions can be elevated. Hence, alternative scenarios with emissions of from 3 orders of magnitude less to 1 order of magnitude more than the limit (Samaras et al., 2022) are also included in the comparison. A typical heating time of an AH, ½ h, and the driving length of the Worldwide harmonized Light vehicles Test Cycle (WLTC), 23.25 km, are used in comparing the particle number emitted by an AH and by an engine. The WLTC length is used to approximate a typical commuting distance. It can be observed that the proportion of total particles emitted by the AH is tens of percent (81% for gasoline and 46% for diesel, in the baseline case). The typical heating time results in a similar number of emitted particles to driving the length of 97 km (gasoline) or 20 km (diesel). However, notable is that these lengths can be even thousands of kilometers for vehicles emitting less than the limit in the regulation. It should also be noted that, in order to decrease the engine warm-up time, AHs usually activate automatically with the engine start and can continue their operation after the engine starts in cold conditions. Therefore, the contributions of AHs to the total emissions can be even higher as the heating times can be longer and as the emissions by AHs can still continue when driving.

3.5. Ignition and shutdown emission compared to steady state emissions

Both gasoline- and diesel-operated AHs displayed the highest concentrations right after the start and the end of combustion, whereas instantaneous concentrations approached nearly steady values during steady operation, of which duration depends on user preferences. Especially since Euro 5 b emission standard diesel vehicles that are all equipped with a DPF, the AH emissions are highlighted in relation to the very low particle levels found in tailpipe.

3.6. Effect of AH heating on vehicle net emissions

To assess the effectiveness of AH heating, emissions caused by preheating must be weighed against improvements in vehicle fuel consumption, engine wear, and emissions compared to cold-start emissions. Since the heating cycle has significantly higher emissions during the start and shutdown phases of combustion, those parts could be considered “fixed costs” of heating with “variable cost” dependent on heating time. Ignition emissions are assumed to depend on outside temperature before ignition, and shutdown emission is likely affected by heating time. Based on these assumptions, the net emissions of AH heating could be estimated by equation

$$y(T,T_{out},t,s) = I(T) + S(t) + Et - R(t,s,T_{out})$$

Where T is the initial vehicle temperature before preheating, T_{out} is outside temperature during post heating driving, t is the post-ignition heating time, s is the distance traveled after heating, $I(T)$ is the initial-temperature-dependent ignition emission, $S(t)$ is the shutdown emissions, E is the emission per unit of time during the steady part of the heating cycle, and $R(t,s,T_{out})$ is the reduction of driving emissions due to preheating the engine. The term $R(t,s,T_{out})$ could be measured by comparing vehicle cold-start emissions during driving against emissions from similar drive with vehicle preheated with AH. If terms of the above equation could be accurately estimated from measurements, it would be possible to calculate the optimal heating time for drives of varying lengths and initial temperatures. Different components of emissions will likely behave differently from each other, thus resulting in different optimal heating times for each component of total emissions (e.g., CO_2, PN, BC, and NO_x) requiring some type of combined optimal heating time. That would require a model for weighting comparative importance of reducing different types of emissions. Such a model would enable the calculation of the optimal heating time to minimize the total effects of vehicle and AH emissions. Naturally AHs provide benefits besides fuel and emission economy improvements, for example, heated passenger compartment during winter months, that are hard to mathematically compare against air quality and environmental cost of emissions.

Table 2
Comparison of emissions of the number of non-volatile particles larger than 23 nm. The bold values represent the baseline assumption (driving emissions equal to the limit in European regulation). Other values represent alternative scenarios with 0.001, 0.01, 0.1, or 10 times the limit value for driving emissions.

Fuel	10^{12}/kg_{fuel} emitted by the AH	10^{12}/½h (typical heating time) emitted by the AH	10^{12}/km emitted by driving	10^{12}/23.25 km (WLTC length) emitted by driving	Proportion of particles emitted by the AH (%)	Driving length emitting equal number of particles to the AH (km)
Gasoline	220	58	0.0006	0.014	99.98	97 000
			0.006	0.14	99.8	9700
			0.06	1.4	98	970
			0.6	**14**	**81**	**97**
			6	140	29	9.7
Diesel	48	12	0.0006	0.014	99.9	20 000
			0.006	0.14	99	2000
			0.06	1.4	90	200
			0.6	**14**	**46**	**20**
			6	140	7.9	2.0

4. Conclusions

Experiments for studying the AH-originated emissions were performed under Finnish winter conditions mimicking real-world use for six selected vehicles with original AHs installed, including both gasoline- and diesel-powered heaters. The start-up and shutdown phases of the heating cycle showed the highest particle peaks, while the particle concentrations were stable between these. The particle number, mass and BC emission factors were found to be as high as 590×10^{12} kg_{fuel}^{-1}, 33 mg kg_{fuel}^{-1} and 18 mg kg_{fuel}^{-1} for gasoline-operated heaters and 560×10^{12} kg_{fuel}^{-1}, 20 mg kg_{fuel}^{-1} and 12 mg kg_{fuel}^{-1} for diesel-operated heaters, respectively. Comparing the AH and tailpipe emissions of particles larger than 23 nm showed that a typical heating cycle emits an equal number of particles to drive dozens or even thousands of kilometers depending on the emission level of the vehicle. The high emission factors from AHs raise the question whether the use of heaters is justified based on the goal of reducing total emissions. Based on our measurements AHs produce amount of particle emissions which would be unacceptable if they were regulated equally with engine emissions. Since environmental effects of emissions are not source-dependent, the AH and engine emissions should be treated equally in emission regulations. Possible solution to high emissions produced by fuel-operated AHs would be emissions aftertreatment devices for AHs aligning with those currently used for engine emissions or use of electric heaters or alternative heating solutions. In order to assess the environmental impact of these notably high emissions from the AHs, additional research on the usage of the devices will be needed. It is clear that the emissions should be under regulation but defining the level of regulation needs quantification.

Associated content

Supporting Information. Supporting information contains more details on (I) investigation of the effects of coagulation and diffusion in the sampling lines on particle size distributions, and (II) emission factors and their internal variance during measured heating cycle.

Funding sources

This research is part of the “AHMA” project funded by the Jane and Aatos Erkko’s Foundation and the Academy of Finland project “EFFi” grant No. 322120. S. Mi. Is supported by the Academy of Finland competitive funding to strengthen university research profiles (PROFI) for the University of Eastern Finland (grant No. 325022). S. Ma. acknowledges funding from the Kone Foundation. This research has received support from the Academy of Finland Flagship Programme “ACCC” (Grant numbers 337550 and 337551).

CRediT authorship contribution statement

Henri Oikarinen: Conceptualization, Methodology, Software, Formal analysis, Writing – original draft, Writing – Revised manuscript, Visualization. **Miska Olin:** Conceptualization, Methodology, Software, Investigation, Resources, Data curation, Writing – original draft, Writing – Revised manuscript, Visualization, Supervision, Project administration. **Sampsa Martikainen:** Conceptualization, Methodology, Investigation, Writing – original draft. **Ville Leinonen:** Conceptualization, Methodology, Writing – original draft. **Santtu Mikkonen:** Conceptualization, Methodology, Investigation, Resources, Data curation, Writing – original draft, Writing – Revised manuscript, Supervision, Project administration, Funding acquisition. **Panu Karjalainen:** Conceptualization, Methodology, Investigation, Resources, Data curation, Writing – original draft, Writing – Revised manuscript, Supervision, Project administration, Funding acquisition.

Declaration of competing interest

The authors declare that they have no known competing financial interests or personal relationships that could have appeared to influence the work reported in this paper.

Acknowledgments

We acknowledge Dr. Anssi Arffman and Dr. Antti Rostedt for their assistance in providing vehicles for the tests.

Appendix A. Supplementary data

Supplementary data to this article can be found online at https://doi.org/10.1016/j.aeaoa.2022.100189.

References

Burnett, R., Chen, H., Szyszkowicz, M., Fann, N., Hubbell, B., Pope, C.A., Apte, J.S., Brauer, M., Cohen, A., Weichenthal, S., Coggins, J., Di, Q., Brunekreef, B., Frostad, J., Lim, S.S., Kan, H., Walker, K.D., Thurston, G.D., Hayes, R.B., Lim, C.C., Turner, M.C., Jerrett, M., Krewski, D., Gapstur, S.M., Diver, W.R., Ostro, B., Goldberg, D., Crouse, D.L., Martin, R.V., Peters, P., Pinault, L., Tjepkema, M., Van Donkelaar, A., Villeneuve, P.J., Miller, A.B., Yin, P., Zhou, M., Wang, L., Janssen, N. A.H., Marra, M., Atkinson, R.W., Tsang, H., Thach, T.Q., Cannon, J.B., Allen, R.T., Hart, J.E., Laden, F., Cesaroni, G., Forastiere, F., Weinmayr, G., Jaensch, A., Nagel, G., Concin, H., Spadaro, J.V., 2018. Global estimates of mortality associated with longterm exposure to outdoor fine particulate matter. Proc. Natl. Acad. Sci. U.S. A. 115, 9592–9597. https://doi.org/10.1073/pnas.1803222115.

Chowdhury, S., Pozzer, A., Haines, A., Klingmüller, K., Münzel, T., Paasonen, P., Sharma, A., Venkataraman, C., Lelieveld, J., 2022. Global health burden of ambient PM2.5 and the contribution of anthropogenic black carbon and organic aerosols. Environ. Int. 159, 107020 https://doi.org/10.1016/j.envint.2021.107020.

Dieselnet, 2015. Emission Standards: Europe: Cars and Light Trucks [WWW Document]. Dieselnet. URL. http://www.dieselnet.com/standards/eu/ld.php#stds.

EUR-Lex - 42010X0630(08) - EN - EUR-Lex [WWW Document], n.d. URL https://eur-lex.europa.eu/legal-content/EN/TXT/?uri=CELEX%3A42010X0630%2808%29 (accessed 2.3.22).

Forster, P.M., Storelvmo, T., Armour, K., Collins, W., Dufresne, J.L., Frame, D., Lunt, D.J., Mauritsen, T., Palmer, M.D., Watanabe, M., Wild, M., Zhang, H., 2021. Chapter 7: the Earth’s energy budget, climate feedbacks, and climate sensitivity. In: Masson-Delmotte, V., Zhai, P., Pirani, A., Connors, S.L., Péan, C., Berger, S., Caud, N., Chen, Y., Goldfarb, L., Gomis, M.I., Huang, M., Leitzell, K., Lonnoy, E., Matthews, J. B.R., Maycock, T.K., Waterfield, T., Yelekçi, O., Yu, R., Zhou, B. (Eds.), Climate Change 2021: the Physical Science Basis. Contribution of Working Group I to the Sixth Assessment Report of the Intergovernmental Panel on Climate Change. Cambridge University Press (in press).

Gentner, D.R., Jathar, S.H., Gordon, T.D., Bahreini, R., Day, D.A., El Haddad, I., Hayes, P. L., Pieber, S.M., Platt, S.M., De Gouw, J., Goldstein, A.H., Harley, R.A., Jimenez, J.L., Prévôt, A.S.H., Robinson, A.L., 2017. Review of urban secondary organic aerosol formation from gasoline and diesel motor vehicle emissions. Environ. Sci. Technol. 51, 1074–1093. https://doi.org/10.1021/acs.est.6b04509.

Giechaskiel, B., Maricq, M., Ntziachristos, L., Dardiotis, C., Wang, X., Axmann, H., Bergmann, A., Schindler, W., 2014. Review of motor vehicle particulate emissions sampling and measurement: from smoke and filter mass to particle number. J. Aerosol Sci. 67, 48–86. https://doi.org/10.1016/j.jaerosci.2013.09.003.

Glarborg, P., Miller, J.A., Ruscic, B., Klippenstein, S.J., 2018. Modeling nitrogen chemistry in combustion. Prog. Energy Combust. Sci. 67, 31–68. https://doi.org/10.1016/j.pecs.2018.01.002.

Hadley, O.L., Kirchstetter, T.W., 2012. Black-carbon reduction of snow albedo. Nat. Clim. Change 2, 437–440. https://doi.org/10.1038/nclimate1433.

Högström, R., Karjalainen, P., Yli-Ojanperä, J., Rostedt, A., Heinonen, M., Mäkelä, J.M., Keskinen, J., 2012. Study of the PM gas-phase filter artifact using a setup for mixing diesel-like soot and hydrocarbons. Aerosol Sci. Technol. 46, 1045–1052. https://doi.org/10.1080/02786826.2012.689118.

Karjalainen, P., Nikka, M., Olin, M., Martikainen, S., Rostedt, A., Arffman, A., Mikkonen, S., 2021. Fuel-operated auxiliary heaters are a major additional source of vehicular particulate emissions in cold regions. Atmosphere 12, 1105. https://doi.org/10.3390/atmos12091105.

Karjalainen, P., Pirjola, L., Heikkilä, J., Lähde, T., Tzamkiozis, T., Ntziachristos, L., Keskinen, J., Rönkkö, T., 2014. Exhaust particles of modern gasoline vehicles: a laboratory and an on-road study. Atmos. Environ. 97, 262–270. https://doi.org/10.1016/j.atmosenv.2014.08.025.

Keskinen, J., Rönkkö, T., 2010. Can real-world diesel exhaust particle size distribution be reproduced in the laboratory? A critical review. J. Air Waste Manag. Assoc. 60, 1245–1255. https://doi.org/10.3155/1047-3289.60.10.1245.

Müller, E.A., Onder, C.H., Guzzella, L., Kneifel, M., 2009. Optimal control of a fuel-fired auxiliary heater for an improved passenger vehicle warm-up. Control Eng. Pract. 17, 664–675. https://doi.org/10.1016/j.conengprac.2008.10.017.

Ntziachristos, L., Giechaskiel, B., Pistikopoulos, P., Samaras, Z., Mathis, U., Mohr, M., Ristimäki, J., Keskinen, J., Mikkanen, P., Casati, R., Scheer, V., Vogt, R., 2004.

Performance evaluation of a novel sampling and measurement system for exhaust particle characterization. In: SAE Technical Papers. https://doi.org/10.4271/2004-01-1439.

Pearson, R.K., Neuvo, Y., Astola, J., Gabbouj, M., 2016. Generalized Hampel filters. EURASIP J. Appl. Signal Process. 2016, 87. https://doi.org/10.1186/s13634-016-0383-6.

Rönkkö, T., Virtanen, A., Kannosto, J., Keskinen, J., Lappi, M., Pirjola, L., 2007. Nucleation mode particles with a nonvolatile core in the exhaust of a heavy duty diesel vehicle. Environ. Sci. Technol. 41, 6384–6389. https://doi.org/10.1021/es0705339.

Rönkkö, T., Virtanen, A., Vaaraslahti, K., Keskinen, J., Pirjola, L., Lappi, M., 2006. Effect of dilution conditions and driving parameters on nucleation mode particles in diesel exhaust: laboratory and on-road study. Atmos. Environ. 40, 2893–2901. https://doi.org/10.1016/j.atmosenv.2006.01.002.

Samaras, Z., Rieker, M., Papaioannou, E., van Dorp, W.F., Kousoulidou, M., Ntziachristos, L., Andersson, J., Bergmann, A., Hausberger, S., Keskinen, J., Karjalainen, P., Martikainen, S., Mamakos, A., Haisch, C., Kontses, A., Toumasatos, Z., Landl, L., Bainschab, M., Lähde, T., Piacenza, O., Kreutziger, P., Bhave, A.N., Lee, K.F., Akroyd, J., Kraft, M., Kazemimanesh, M., Boies, A.M., Focsa, C., Duca, D., Carpentier, Y., Pirim, C., Noble, J.A., Lancry, O., Legendre, S., Tritscher, T., Spielvogel, J., Horn, H.G., Pérez, A., Paz, S., Zarvalis, D., Melas, A., Baltzopoulou, P., Vlachos, N.D., Chasapidis, L., Deloglou, D., Daskalos, E., Tsakis, A., Konstandopoulos, A.G., Zinola, S., Di Iorio, S., Catapano, F., Vaglieco, B.M., Burtscher, H., Nicol, G., Zamora, D., Maggiore, M., 2022. Perspectives for regulating 10 nm particle number emissions based on novel measurement methodologies. J. Aerosol Sci. 162, 105957 https://doi.org/10.1016/j.jaerosci.2022.105957.

Wang, J.M., Jeong, C.H., Zimmerman, N., Healy, R.M., Evans, G.J., 2018. Real world vehicle fleet emission factors: seasonal and diurnal variations in traffic related air pollutants. Atmos. Environ. 184, 77–86. https://doi.org/10.1016/j.atmosenv.2018.04.015.

Wang, X., Grose, M.A., Caldow, R., Osmondson, B.L., Swanson, J.J., Chow, J.C., Watson, J.G., Kittelson, D.B., Li, Y., Xue, J., Jung, H., Hu, S., 2016. Improvement of Engine Exhaust Particle Sizer (EEPS) size distribution measurement - II. Engine exhaust particles. J. Aerosol Sci. 92, 83–94. https://doi.org/10.1016/j.jaerosci.2015.11.003.

Wihersaari, H., Pirjola, L., Karjalainen, P., Saukko, E., Kuuluvainen, H., Kulmala, K., Keskinen, J., Rönkkö, T., 2020. Particulate emissions of a modern diesel passenger car under laboratory and real-world transient driving conditions. Environ. Pollut. 265 https://doi.org/10.1016/j.envpol.2020.114948.